Performance of code tracking loops in ultra-tight GPS/INS/PL integration

Ravindra Babu, Jinling Wang, Andrew Dempster
School of Surveying and Spatial Information Systems
University of New South Wales

Tel: 61-2-93854203
Fax: 61-2-93137493

Emails: **z3073030@student.unsw.edu.au**;
Jinling.Wang@unsw.edu.au

ABSTRACT: With its several inherent advantages, an ultra-tightly coupled GPS/INS/PL system will have a dramatic increase in both commercial and defence applications. Integrating the correlator measurements, *I* (in-phase) and *Q* (quadrature), with position, velocity and attitude from INS in a Kalman filter characterises this type of system. The Doppler feedback derived from the corrected INS is then fed back to the carrier-tracking loop to remove the dynamics from the GPS/PL ranging signal, thereby reducing the carrier tracking bandwidth. This reduction in bandwidth is the principal reason behind its popularity. Some of the applications where this system can be used are: dynamic scenarios, weak signal conditions, interference & jamming environments, etc.

Although the code loops are not directly aided by the INS-derived Doppler in an ultra-tightly coupled system, accurate knowledge of Doppler information from INS results in better code thresholds. This improvement in threshold further increases the accuracy of raw measurements and also the jamming immunity. Normally the code loop bandwidth is about 1 to 3 Hz in an unaided case, but in this type of integrated system the bandwidth is typically less than 1 Hz as the code dynamics are mitigated as well.

In this paper, the mathematical analysis pertaining to code dynamics is presented. An E-L/E+L discriminator is utilised as a software-based receiver is used for the experiments. Various trajectories with different dynamics are generated and the code-tracking loops are tested, and the results show substantial improvement in the code thresholds.

INTRODUCTION:

Integrating the receiver tracking loops measurements, I (in-phase) and Q (quadrature), with inertial sensor variables, P (Position), V (Velocity) and A (Attitude), is generally referred to as 'ultra-tight GPS/INS integration'.

GPS and Inertial Navigation Systems have been integrated in loosely- and tightly-coupled architectures over the past two decades. Nevertheless, the advantages that are obtained from ultra-tight integration far outweigh the advantages from the previous two architectures. The principle of ultra-tight integration is: if the dynamics on the GPS signal can be measured by an additional sensor such as an INS, then this information can be integrated within the receiver tracking loops, resulting in significant reduction in tracking bandwidth (especially the carrier tracking bandwidth). This bandwidth reduction has a number of advantages: signal-to-noise ratio improvement, interference reduction, reduction in non-coherent integration period, etc (Beser et al., 2002). In addition to these advantages, the ultra-tight architecture has another advantage: reduced correlations in the GPS measurements, I and Q; and this has the effect of reduced dimensions in the integration Kalman filter.

The conventional tracking loops are sensitive to receiver dynamics resulting in loss-of-lock when the dynamics exceed a certain threshold (Cahn, 1977). In a stand-alone receiver, the carrier-tracking bandwidth is of the order of 12 to 18 Hz, and the code-tracking bandwidth is 1 to 4 Hz (Ward, 1998; Farrell, 1999). To reduce the dynamic stress error, in general the bandwidths have to be increased, which degrades the signal quality due to increased thermal noise. Therefore, the tracking loop bandwidth becomes an optimal parameter in receiver design. However, without sacrificing the quality of signal measurements, the bandwidth can still be reduced by using inertial aiding. If the Doppler derived from an INS can reflect the Doppler on the GPS signals, within the limitations of calibration errors, then it can be integrated with the NCO of the carrier-tracking loops, reducing the dynamics on the GPS signals, and yielding reduced bandwidths. This will also result in reduced code-tracking bandwidth due to the carrier-aiding of the code-tracking loops.

Though the code-tracking loop is not as sensitive as the carrier tracking loops to dynamics, due to its low frequency, nevertheless the inertial aiding results in bandwidth improvement. The code loop performance is important especially in systems that use code phase for positioning. The errors that affect the carrier loop, such as thermal noise and dynamic stress errors, also affect the code loop. Therefore, the dynamic performance of the DLL becomes important when the receiver is subjected to dynamics. During dynamic scenarios, when the cumulative error in the DLL transgresses the threshold, then the system eventually loses lock. One way to mitigate this is to increase the threshold, which also increases the false locks. The other is to reduce the dynamic stress error by using aiding sensors such as an INS.

A normalised discriminator algorithm is adopted for the experiments, as a Software Receiver is used here. This paper shows the effect of dynamics on code loops by simulating trajectories with different dynamics. Related mathematics is also provided. The dynamic effect on code-tracking bandwidth is also analysed. Finally, simulation experiments are conducted to validate the theoretical arguments.

Ultra-tight Integration Architecture

Ultra-tight integration refers to the integration of correlator quadrature measurements, I and Q, with INS variables, P, V and A. The measurements from both these systems are integrated in a complementary Kalman filter, which calibrates the inertial sensor errors and removes from the subsequent inertial measurements (Brown & Hwang, 1997, Maybeck, 1979; Wang, 2001). Unlike in loosely- and tightly-coupled architectures, where the relationships between the measurements and states are relatively simple, in the ultra-tight architecture the relationship is quite complex. Here, the relationship between measurements and states is through phase and frequency errors.

The *I and Q* measurements from N channels are integrated with the position, velocity and attitude of the INS in a complementary Kalman filter, as shown in Figure 1. The INS information is converted to I and Q by the I, Q predictor block and differenced from the receiver I, Q measurements to generate the GPS and INS errors which drive the Kalman filter. In a conventional GPS receiver, the code and carrier loops of each channel generate corrections to align the locally-generated signals with the incoming signal based on their respective discriminator functions. These correction signals are then low-pass filtered to remove any high frequency noise and higher order terms on them. The bandwidth is usually of the order of 5 to 15 Hz for low dynamic signals (Jwo, 2001), and greater than 20 Hz for high dynamic signals. Higher bandwidths result in a degradation of the measurements due to the increased thermal noise. Ultra-tight tracking loops (tracking loops aided with INS-derived Doppler) can circumvent this problem by tracking high dynamic signals without increasing the bandwidth. In fact, the bandwidth can be reduced to even less than 3 Hz under high dynamic scenarios (Sennott, 1992; Sennott, 1997).

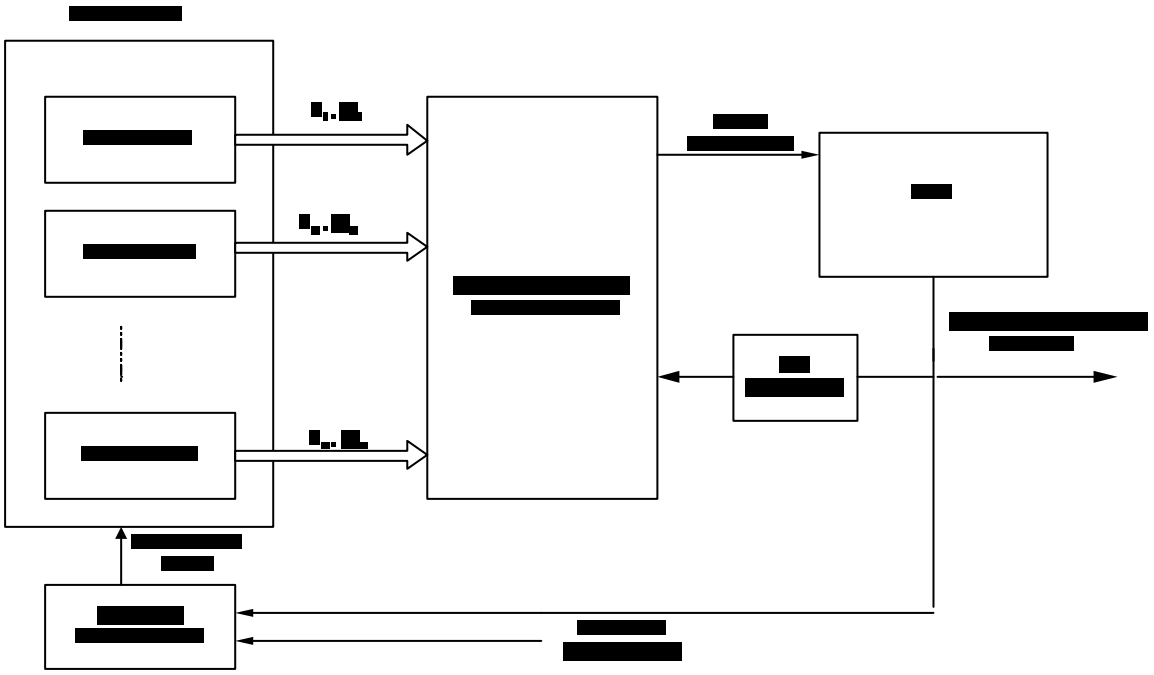

Figure 1 Ultra-tight integration architecture

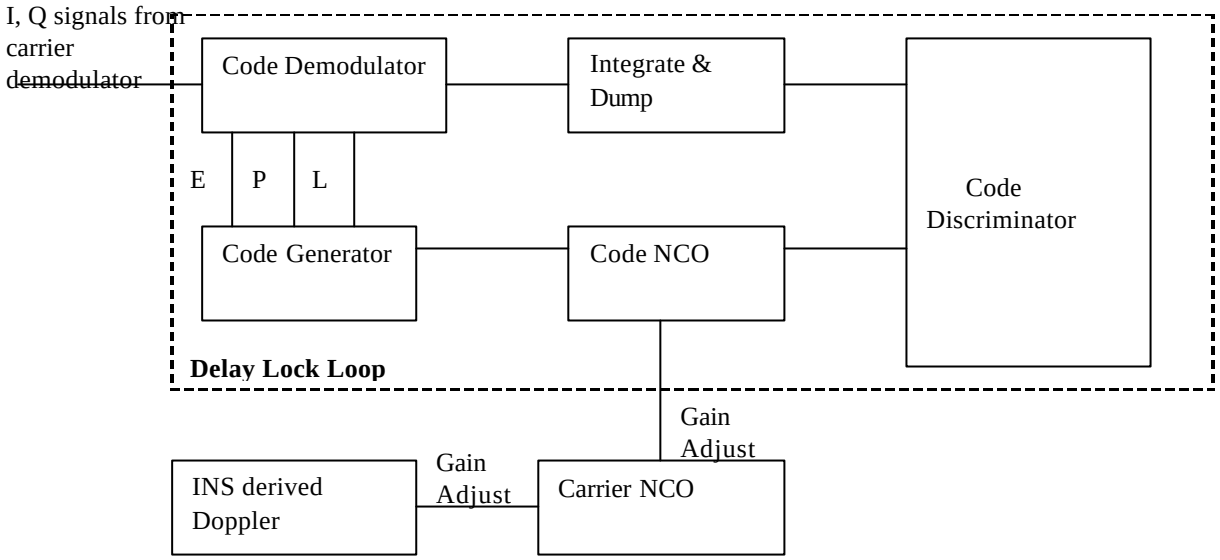

Figure 2. Ultra-tight Code Tracking Loop

The fundamental principle behind ultra-tight integration is: if the INS can measure the same vehicle dynamics as the GPS receiver and somehow be integrated within the tracking loops (as shown in Figure 2), then the dynamics on the GPS signal as seen by the receiver tracking loops can be reduced significantly. Ignoring multipath and ionospheric effects, the majority of the residual dynamics on the GPS signal will then be due to the local oscillator offsets and estimation errors in the INS-derived Doppler. This composite GPS signal (with reduced dynamics) is multiplied with the locally-estimated signals to generate the quadrature I and Q signals. These quadrature signals are used by the discriminator functions to generate correction signals to align the local oscillators to the incoming signal. In ultra-tight integration, the I *and* Q signals which form the measurements in the Kalman filter estimate the inertial sensor errors during the measurement update process, and subsequently remove them from the INS measurements. Using the almanac or ephemeris information, the Doppler signal is derived from the INS and integrated with the carrier-tracking loops. As GPS is considered a sensor in this architecture, the INS error states can be estimated even with less than four satellites.

Ultra-tight Code Tracking Loop Analysis

Two tracking loops, the CPLL and DLL, work concurrently to demodulate the pseudo-random noise code and carrier frequency to extract the 50 Hz navigation data. User position is calculated from code phase measurements, whereas velocity is calculated from the carrier frequency measurements. Generally, the code loop is less sensitive to dynamics than the carrier loop owing to its low frequency characteristics, and also due to carrier aiding. The carrier aiding virtually removes most of the dynamics from the measurements that enter the code-tracking loop. Therefore the bandwidth of the code-tracking loop can be maintained at about 1 to 4 Hz. If the carrier loops loses lock, usually the code loop will also lose lock (Kaplan, 1996).

The closed loop transfer function of the code-tracking loop shown in Figure 2 is given as:

$$H(s) = \frac{K_0 K_d F(s)}{s + K_0 K_d F(s)} \tag{1}$$

where K_0 is the NCO gain, K_d is the discriminator gain, $F(s)$ is the loop filter transfer function. Depending on the dynamics on the received signal the order of the filter is adjusted. However, due to carrier aiding, a first order delay locked loop is usually employed.

The Delay Lock Loop is characterised by Code Generator, Code NCO, and Discriminator algorithms. The Code Generator generates three different phases in phase quadrature – Early, Prompt and Late which are typically separated by ½ chip spacing. The Early phase is ½ chip advanced with respect to the prompt phase, whereas the late phase is ½ chip retarded with respect to the prompt phase. These three signals are multiplied with the incoming composite signal to identify the code phase starting point in the composite signal. In an ideal scenario, when the prompt phase gets exactly aligned to the

incoming code phase, the prompt arm correlation output results in a triangle with a sharp peak at zero offset and linearly ramping down to zero at 1 chip offset, as shown in Figure 3. Under this condition, the early and late arms will have 3 dB less power than in the prompt arm.

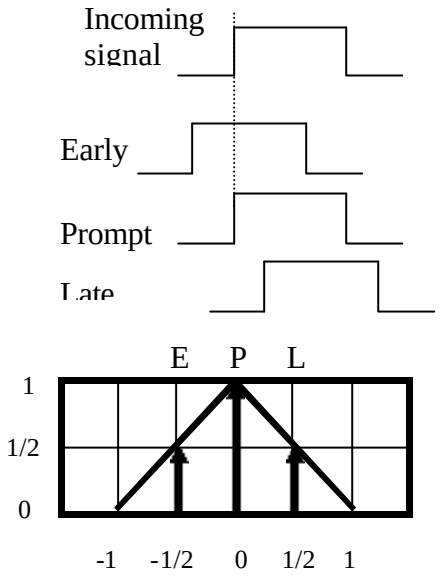

Figure 3. Code Autocorrelation

However, due to finite front-end bandwidth and correlated errors such as multipath, the correlation peak is not sharp but distorted, which degrades the pseudo-range measurements, and eventually the navigation solution. The offsets in the locally-generated code phases with respect to the incoming signal are determined by the code discriminator functions. Ward (1998) proposes four different discriminators, tabulated in Table 1, with each having their own advantages and disadvantages.

The performance of the discriminator transfer functions are shown in Figure 4. As the Normalized envelope is insensitive to amplitude fluctuations, it is the preferred one, especially for Software Receivers. Correlator spacing is an optimal parameter which affects the DLL performance; while wider spacing allows faster acquisition the narrow spacing improves interference and multipath effects (Van, 1992; Gustafson, 2003).

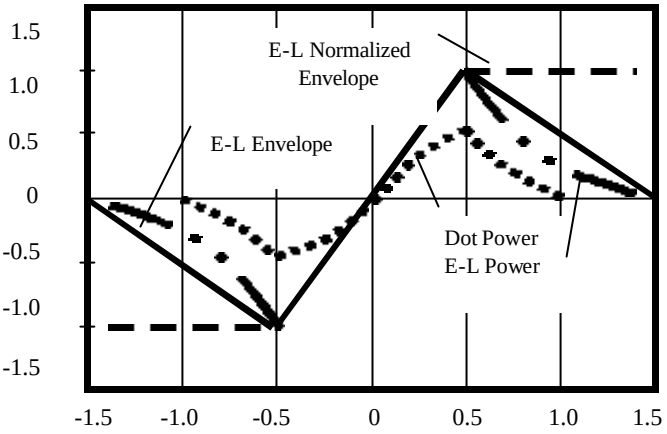

Figure 4. Discriminators output

As a Software Receiver is used for the analysis and experiments in this paper, an E-L Normalized discriminator algorithm is used. The early minus late normalized envelope removes amplitude sensitivity, which provides better performance against pulse-type interference, but demands the highest computational load.

Table 1. Discriminator algorithms

Dot product power	$(I_{ES}-I_{LS})I_{PS}-(Q_{ES}-Q_{LS})Q_{PS}$
Early minus *Late power*	$(I_{ES}^2+Q_{ES}^2)-(I_{LS}^2+Q_{LS}^2)$
Early minus *Late envelope*	$\sqrt{I_{ES}^2+Q_{ES}^2}-\sqrt{I_{LS}^2+Q_{LS}^2}$
Early minus *Late Normalized envelope*	$\dfrac{\sqrt{I_{ES}^2+Q_{ES}^2}-\sqrt{I_{LS}^2+Q_{LS}^2}}{\sqrt{I_{ES}^2+Q_{ES}^2}+\sqrt{I_{LS}^2+Q_{LS}^2}}$

Doppler Analysis

The received carrier Doppler frequency on L1 is given as:

$$f_{rx} = f_{tx}\left(1 - \frac{v_r \vec{a}}{c}\right) \; and \;\; f_{carr} = f_{tx} - f_{rx} \qquad (2)$$

where

$$f_{tx} = 1575.42e6$$
$$v_r = relative velocity$$
$$c = velocity of\ light$$
$$\vec{a} = line\ of\ sight vector$$

The total Doppler on f_{rx} can be factored into:

$$f_{carr} = f_{rel\_vel} + f_{sat\_clk} + f_{rx\_clk} + f_{errors} \qquad (3)$$

where f_{rel_vel} represents the Doppler due to the relative velocity between the satellite and the receiver, f_{sat_clk} represents the Doppler due to satellite clock errors, f_{rx_clk} is due to receiver clock errors, f_{errors} is due to atmospheric and other errors. Due to its lower frequency, the Doppler on the code is 1540 times less than the carrier.

$$f_{code} = f_{carr} / 1540 \qquad (4)$$

The INS measurements can rate-aid the carrier and code-tracking loops to reduce the dynamic stress. The aiding will significantly reduce the loop bandwidths. As a result, the thermal noise and interferences are mitigated, resulting in an improvement in the accuracy of the measurements. The tracking thresholds also can be improved. However, one factors that limits the bandwidth of the loops is how accurately the IMU-derived Doppler measurements can be obtained. Any errors in the calibration of inertial sensor errors by the integration Kalman filter translates to aiding Doppler errors, which in turn limit the bandwidth reduction. The INS estimated Doppler frequency is given as:

$$f_{INS} = f_{rel\_vel} + f_{sys\_errors} + f_{stoc\_errors} \qquad (5)$$

where f_{sys_errors} is due to residual inertial bias from the integration Kalman filter, and f_{stoc_errors} is due to the stochastic errors from the inertial sensors.

The INS-aiding cancels the Doppler due to relative velocity leading to:

$$f^{carr}_{ultra-tight} = f_{carr} - f_{INS}$$
$$= f_{sat\_clk} + f_{rx\_clk} + f_{errors} - f_{sys\_errors} - f_{stoc\_errors} \qquad (6)$$

As the carrier frequency aids the code loop, the code Doppler is given as:

$$f^{code}_{ultra-tight} = \frac{f^{carr}_{ultra-tight}}{1540} \qquad (7)$$

Therefore, the code-tracking loop needs to track this Doppler for continuous tracking.

Code Tracking Loop Error Analysis

The two dominant errors in the code-tracking loop are thermal jitter and dynamic stress error. While the former is associated with the bandwidth, the latter is associated with the signal dynamics. A higher bandwidth usually results in increased thermal noise and reduced dynamic stress errors, whereas the contrary occurs with lower bandwidths. Therefore the bandwidth needs to be optimised for thermal and dynamic performance. For the loop to be in track, the 3-sigma errors of the combined thermal and dynamic errors should not transcend the correlator spacing, d, in chips which is denoted as:

$$3s_{DLL} = 3s_{tDLL} + R_e \le d \qquad (chips) \qquad (8)$$

The thermal error is given as:

$$s_{tDLL} = \left[\frac{B_L d}{2c/n_0}\left(1 + \frac{2}{T(2-d)c/n_0}\right)\right]^{1/2} \qquad (9)$$

where B_L is the loop bandwidth, d is the chip spacing, T is the pre-detection integration period, and

$$c/n_0 = (\text{SNR})\ B_L\ (\text{Ratio-Hz})$$
$$C/N_0 = 10\log_{10}(c/n_0)\ (dB-Hz) \qquad (10)$$

The dynamic stress error is given as:

$$R_e = \frac{dR^n / dt^n}{w_0^n} \qquad (11)$$

where the line-of-sight dynamics dR^n / dt^n is expressed in chips/sec. A rule-of-thumb states that the three-sigma code noise should not exceed 0.5 chips. Therefore, the 1-sigma code noise should not exceed $1/6^{th}$ of the chip length. Figure 5 shows the thermal error, and the dynamic stress error at receiver dynamics of 1g and the total errors.

It can be seen from the figure that the dynamic stress error is less than the thermal error, and the combined errors are less than the threshold at signal levels greater than 25 (dB-Hz). Note that a second order loop is used for the experiments.

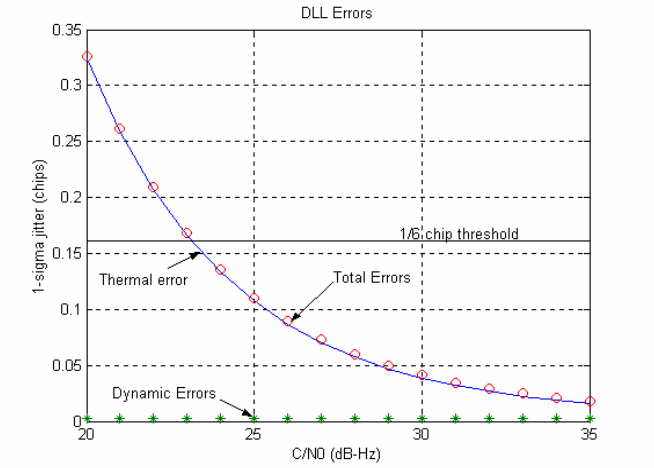

Figure 5. DLL Errors (Thermal, Dynamic and Total)

Simulations & Results

Simulation experiments were carried out to test the performance of the code-tracking loops in the ultra-tightly integrated mode. A reference trajectory shown in Figure 6 was generated using GPSoft™.

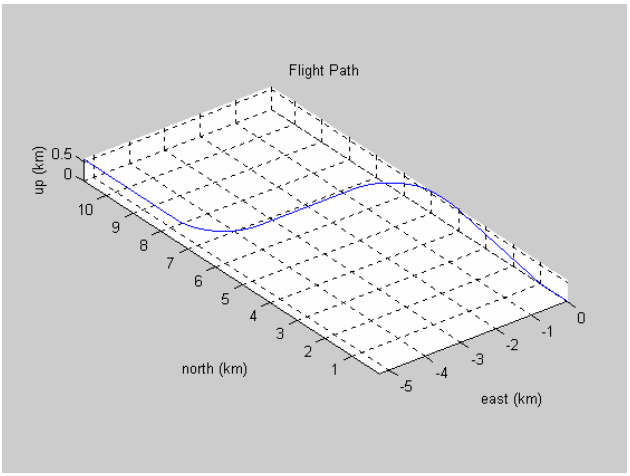

Figure 6. Receiver Trajectory

The trajectory comprises the following segments: acceleration, pitch up, roll, 90 deg turns, straight levelling. Inertial sensor measurements are derived from this trajectory and added with 10.0 mg acc. bias and 1.0 deg/sec gyro bias. Though the integration Kalman filter calibrates these errors, nevertheless there is a residual which produces errors in the INS-derived Doppler. The residual also limits the carrier-tracking loop bandwidth reduction. GPS signals at the receiver antenna are simulated based on this trajectory ignoring atmospheric errors and multipath.

The DLL is carrier-aided for effective removal of the dynamics that enter it. As a result of aiding, the loop order can be set to 1 which is unconditionally stable. A threshold is set for the Delay Lock Loop to indicate when the prompt channel aligns to the composite incoming signal. The threshold is based on the expected dynamics, and the associated statistical properties of the signal. It is calculated based on the formula:

$$threshold = s_n \sqrt{-2 \ln P_{fa}} \qquad (12)$$

where s_n is noise power, P_{fa} is the probability of false alarm, and $\ln$ is the natural algorithm. The pre-detection integration interval is defined as 1 msec.

The experiments are performed in both conventional as well as in ultra-tight mode to verify the code-loop performance. Firstly, in conventional mode the carrier-tracking bandwidth is set at 13 Hz, code-tracking bandwidth at 2 Hz, and the chip spacing at 0.5 chips. For the trajectory shown in Figure 6, the code power results are shown in Figure 7.

Figure 7. Carrier BW = 13 Hz, Code bandwidth = 2 Hz, Code spacing = 0.5 chip

The plot in Figure 7 shows that the code-tracking loops lose lock in the conventional mode. The carrier-tracking bandwidth is then set at 13 Hz, code-tracking bandwidth at 1 Hz and the chip spacing to 0.25 and the experiment is repeated. The results are plotted in Figure 8.

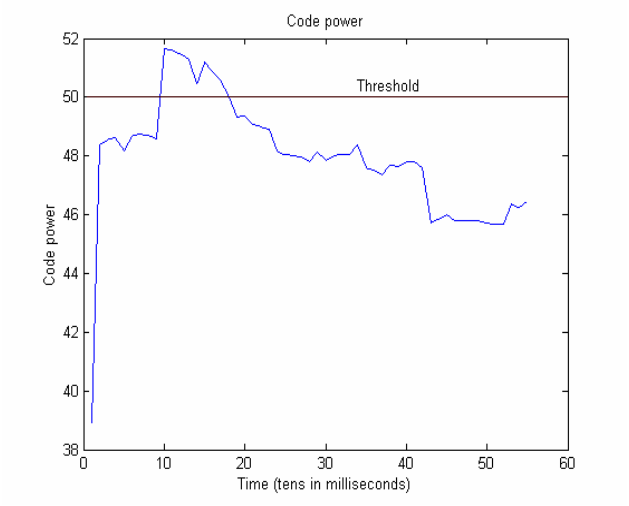

Figure 8. Carrier BW =13 Hz, code BW = 1 Hz, chip spacing = 0. 25 chips

The results show that not only do the code loops lose lock, but that the power also degrades considerably.

Now the receiver is configured in the ultra-tight mode where the tracking loops are aided by the INS-derived Doppler. The experiment is repeated again with the carrier-tracking bandwidth at 3 Hz, the code loop bandwidth set to 1 Hz, and chip spacing of 0.25 chips. The results plotted in Figure 9 show that the code loops perform well in dynamic situations when the loops are configured in the ultra-tight mode.

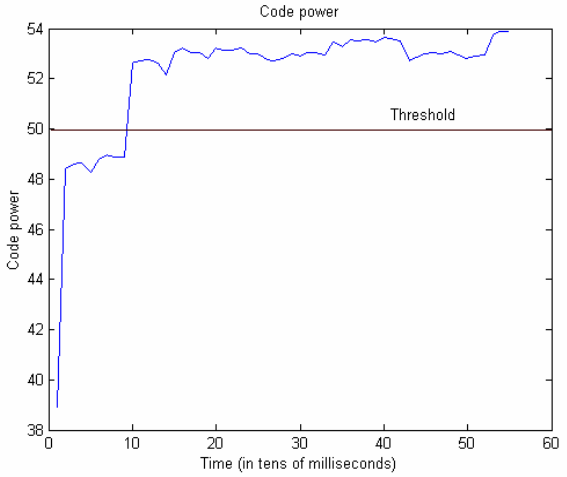

Figure 9. Carrier BW = 3 Hz, code BW = 1 Hz, chip spacing = 0.25 chips

Figure 12 shows that in the ultra-tight mode, the threshold improves, while in conventional tracking loops lose lock during dynamic conditions, as shown in Figure 9. In the ultra-tight mode they remain in lock even with reduced bandwidth due to reduction of dynamics.

Conclusion

The performance of the code-tracking loop is critical in dynamic scenarios as any degradation in its performance may lead to position degradation, or may even result in complete loss-of-lock. Configuring the tracking loops in the ultra-tight mode improves the overall performance when the receiver is subjected to dynamics. The INS-derived Doppler mitigates the dynamic errors so that the loop bandwidths can be reduced to improve the signal-to-noise ratio. The mathematical analysis pertaining to code dynamics is presented in this paper. Simulation experiments are performed to test the validity of the hypothesis, and the results show that an improvement can be obtained in tracking loop performance when integrating the receiver tracking loops with INS-derived Doppler.

Acknowledgement

This Research is supported by an ARC (Australian Research Council) – Discovery Research Project on 'Robust Positioning Based on Ultra-tight Integration of GPS, Pseudolite and Inertial Sensors'.

References

Beser, J., Alexander, S., Crane, R., Rounds, S., Wyman, J., & Baeder, B., (2002) Trunav^{TM}: A Low-Cost Guidance/Navigation Unit Integrating a SAASM-based GPS and MEMS IMU in a Deeply Coupled Mechanization. *15th Int. Tech. Meeting of the Satellite Division of the U.S. Inst. of Navigation*, Portland, OR, 24-27 September, 545-555.

Brown, R.G., & Hwang, P.Y.C., (1997) Introduction to Random Signals and Applied Kalman Filtering. 3rd edition, *John Wiley & Sons*, Boston.

Cahn, R.C., Leimer, D.K., Marsh, C.L., Huntowski, F.J., & Larue, G.D., (1977) Software Implementation of a PN Spread Spectrum Receiver to Accommodate Dynamics. *IEEE Transactions on communications*, 25 (8) pp.832-839.

Farrell, J.A., & Barth, M., (1999) The Global Positioning System and Inertial Navigation. *McGraw-Hill* (ISBN-0-07-022-45-X).

Gustafson, D., & Dowdle, J., (2003) Deeply Integrated Code Tracking: Comparative Performance Analysis. *16th Int. Tech. Meeting of the Satellite Division of the U.S. Inst. of Navigation, Portland*, OR, 9-12 September, 2553-2561.

Campanile, J., Detachment, N., Nasuti, T., Nigro. J., Engelhart., (1992) GPS Acquisition Performance in the Presence of Jamming. *10th Int. Tech. Meeting of the Satellite Division of the U.S. Inst. of Navigation*, Kansas City, Missouri, 16-19 September, 265-274.

Jwo D.-J., (2001) Optimization and Sensitivity Analysis of GPS Receiver Tracking Loops in Dynamic Environments. *IEE Proceedings of Radar, Sonar Navigation*, 148, 241-250.

Jee, G.I., Kim, H.S., Lee, Y.J., Park, C.G., (2002) A GPS C/A Code Tracking Loop Based on Extended Kalman Filter with Multipath Mitigation

Kaplan, E. D., (1996) Understanding GPS Principles and Applications. *Mobile Communications Series, Artech House*, Boston, London.

Maybeck, P. S., (1979) Stochastic Models, Estimation, and Control – Volume I. Academic Press Inc., New York.

Sennott, J.W., & Senffner, D., (1992) The Use of Satellite Geometry for Prevention of Cycle Slips in a GPS Processor. *Navigation, Journal of the Institute of the Navigation*, 39, 217-235.

Sennott, J., & Senffner, D., (1997) Robustness of Tightly Coupled Integrations for Real-Time Centimeter GPS Positioning. *10th Int. Tech. Meeting of the Satellite Division of the U.S. Inst. of Navigation*, Kansas City, Missouri, 16-19 September, 655-663.

Wang, J., Dai, L., Tsuiji, T., Rizos, C., Grejner-Brzezinska, D., Toth, C., (2001) GPS/INS/Pseudolite Integration: Concepts, Simulation and Testing. *145th Int. Tech. Meeting of the Satellite Division of the U.S. Inst. of Navigation*, Salt Lake City, UT, 11-14 September, 2708-2715.

Wang, J., Lee, H.K., & Rizos, C., (2002) GPS/INS Integration: A Performance Sensitivity Analysis. *Wuhan University Journal of Nature Sciences*, 8(2B), 508-516.

Ward, P., (1998) Performance Comparisons Between FLL, PLL and a Novel FLL-Assisted PLL Carrier Tracking Loop Under RF Interference Conditions, *11th Int. Tech. Meeting of the Satellite Division of the U.S. Inst. of Navigation*, Nashville, Tennessee, 15-18 September, 783-795.

Van, D.A.J., Fenton, P., & Ford, T., (1992) Theory and Performance of Narrow Correlator Spacing in a GPS Receiver. *Navigation: Journal of the Institute of Navigation*, 39, 265-283.